（Project use）

CROSS TOKAI **Experimental Report** J-PARC	承認日 Date of Approval 2016/12/15 承認者 Approver Takenao Shinohara 提出日 Date of Report 2016/11/22
Project No. 2015P0701 Title of experiment Pulsed neutron imaging of the temperature, structure, magnetic field, and elemental identification of a practical product with Energy Resolved Neutron Imaging System. Name of principal investigator Kenichi Oikawa Affiliation J-PARC center, JAEA	Name of instrument scientist Takenao Shinohara Name of Instrument/（BL No.） BL22 Date(s) of experiment(s) 2016/2/28 21:00 - 3/2 9:00 2016/3/2 21:00 - 3/7 9:00 2016/3/15 9:00 - 3/19 9:00 2016/3/19 9:00 - 3/22 9:00

1. Outline of experimental method and results. (Experimental method and results should be reported including sample information such as composition, physical and/or chemical characteristics.)

I. Bragg edge imaging

I. 1 Residual strain and microstructure measurement inside an induction hardened gear studied by neutron Bragg-edge Transmission (BET) imaging

【Purpose】

The purpose of this experiment was to study the two-dimensional (2D) distribution of residual strain and microstructure within an engineering product gear sample.

【Background】

Induction hardening is a heat treatment process used for the surface hardening of steel and other alloy components in industry application, which can be used to selectively harden portions of a sample. This treatment provides excellent mechanical properties such as high wear resistance and fatigue strength without affecting the core and other parts of the component. The residual stress and microstructure greatly influenced by the heat treatment are important for the desired property. The newly developed 2D TOF BET imaging method is a very effective and powerful tool for revealing local variations in elastic strain and microstructure in engineering materials. We applied this technique to investigate the microstructure distribution in a gear sample produced by induction hardening.

【Experiment】

The pulsed neutron transmission imaging experiment was performed at BL22 RADEN in MLF/J-PARC. A gear sample, 104 mm in outer diameter, 52 mm in inner diameter and 10 - 20 mm in thickness, was used for the measurement. In addition, 2 small pieces of gear samples were also prepared, one of which was half thickness of the gear and the other was cut from cross-section of the gear. The carbon content in the steel was about 0.55 wt.%. Figures 1(a) and 1(b) are picture of the measured samples and the experimental setup around the sample, respectively. The transmission of the sample was obtained by measuring the spectra with and without the sample

in front of the 2D detector. Crystalline structural information such as lattice plane spacing, texture variations, crystallite size was obtained by using the spectral analysis code, RITS.

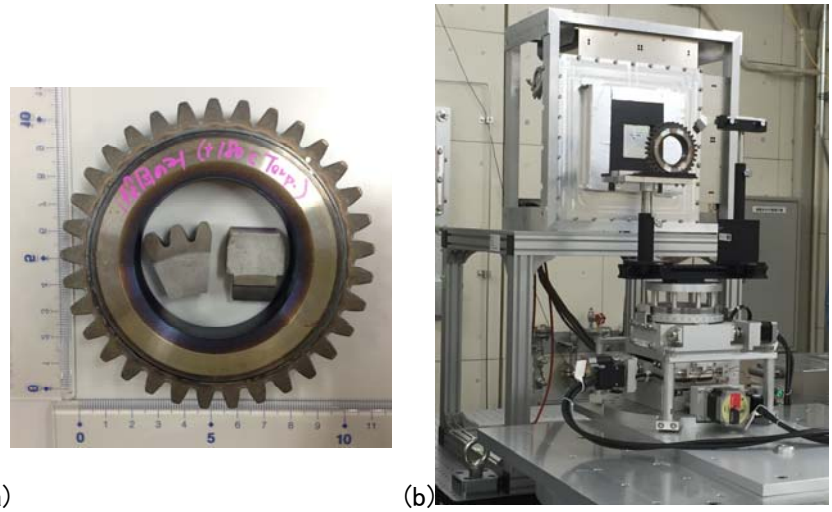

(a) (b)

Figure 1. Photographs of experiment: (a) measured samples, (b) measurement by 2D detector.

【Preliminary Result】

Figures 2(a) shows a radiographic image of the half thickness gear sample. Figure 2 (b) presents the measured and fitted transmission spectra obtained at points A and B indicated in Fig. 2 (a). Enlarged view shown in Figure 2 (c) for the ferrite 110 edges represents the single-edge profile fitting using the RITS code, which provides the lattice plane spacing, d_{110}, where increase of crystal lattice plane spacing and broadening of Bragg-edge were observed in spectrum of point A. Figure 2 (d) shows the 2D map of the determined d_{110}. The crystal lattice plane spacing in the teeth region is obviously larger than body region, indicating the generation of martensitic structure.

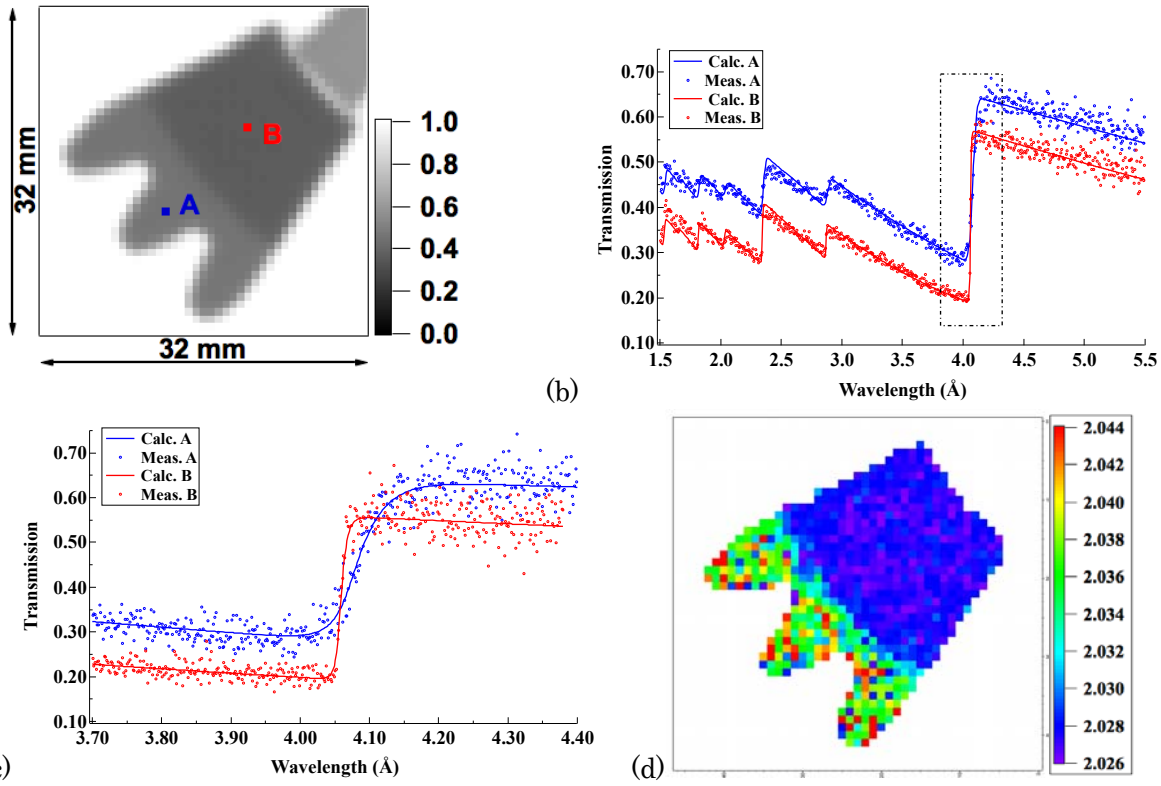

(a) (b) (c) (d)

Figure 2. Example of obtained results: (a) radiographic image of the half thickness gear sample, (b) BET

spectra measured at the points indicated in (a), (c) ferrite 110 single-edge profile fitting and (d) 2D map of the 110 crystal lattice plane spacing, d_{110} (Å).

I. 2 Martensite transformation in austenite steel studied by BET imaging method

【Purpose】

The purpose of this experiment was to study effect of bending deformation (residual stress) and sub-zero treatment (temperature) on nonhomogeneous martensite transformation in metastable austenitic steel.

【Background】

The martensite transformation followed by appropriate tempering treatment is the most effective method to obtain steel products with high strength. Martensite transformation in steel is affected by many parameters, such as chemical composition, external stress, residual strain and temperature. We performed BET imaging measurement on bent plates of a metastable austenitic steel to clarify the martensite transformation induced by nonhomogeneous deformation and subsequent treatment in a sub-zero Celsius temperature range (so called subzero treatment).

【Experiment】

The composition of the metastable austenitic steel for the study was Fe−25wt% Ni−0.4wt% C. Two rectangular-shaped samples with dimensions of 13 × 12 × 250 mm^3 were deformed using a three-point bending process at room temperature (RT). Then, the thickness of the bent samples was machined from ca. 12 mm to 6 mm and 2.5 mm. Subsequently, subzero treatment for the machined samples was applied by isothermal holding at −70°C and −90°C, where the sample thickness was 6 mm and 2.5 mm, respectively. BET imaging experiments were performed at BL22 RADEN of the MLF/J-PARC using the nGEM detector at the position of 23.8 m from the moderator. Samples before and after subzero treatment were measured.

【Preliminary Result】

Figure 3 shows examples of the obtained transmission spectra as a function of neutron wavelength. No martensite was formed in the austenite matrix after bending deformation without subzero treatment. As shown in Fig. 3(a), the presence of austenite and martensite phase could be identified from the transmission spectra for −70°C and −90°C sub-zero treated samples. The nonhomogeneous martensite transformation in −70°C sub-zero treatment sample was confirmed from changes of BET spectra from the outer to inner area of the bent sample as shown in Fig. 3 (b) and 3(c). 2D maps of texture variations, crystallite size, and phase volume fraction were obtained from Bragg-edge spectral analysis using the RITS code. Figure 3 (d) shows the quantitative 2D image of ferrite phase volume fraction for the −70°C sub-zero treated sample. A clear difference of martensite fraction from the outer to the inner zone of the sample is observed. In the center region, only a little martensite forms. However, in the outer zone the martensite fraction reaches about 0.35, which is higher than that in the inner zone. The non-homogeneous martensite formation throughout the whole sample is caused by different stress/strain state in the tensile or compressive region.

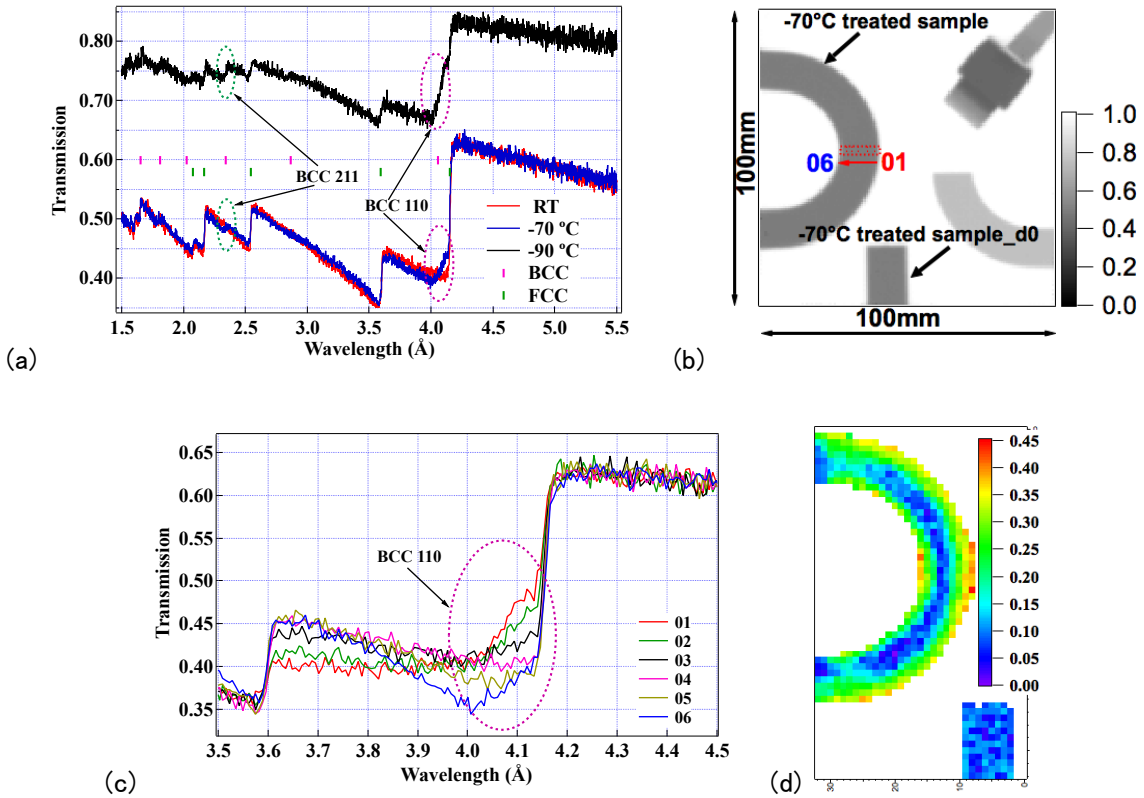

Figure 3 Examples of obtained results: (a) BET spectra for samples before and after subzero treatment, (b) radiographic image, (c) BET spectra from outer zone to inner zone as indicated in (b), and (d) 2D map of martensite volume fraction for sample subzero treated at −70°C.

This work is partially supported by Photon and Quantum Basic Research Coordinated Development Program from the Ministry of Education, Culture, Sports, Science and Technology, Japan.

II. Resonance imaging

【Purpose】

The purpose of this measurement is to obtain experimental data to estimate these parameters aiming to discuss availability of resonance neutron thermometry technique for investigations of lithium ion batteries.

【Background】

Neutron resonance thermometry is a powerful application, and some demonstration measurements have been carried out. However, this technique has not been utilized commonly since such principle parameters as reliability and temporal, spatial and temperature resolutions are not clearly indicated.

【Experiment】

Two-dimensional distributions of neutrons transmitted through a tantalum (0.1mm in thickness) or a tungsten (1 mm in thickness) sheet (Fig. 3 (left)) were measured by the gas-electron multiplier (GEM) neutron detector. Tantalum and tungsten were selected as temperature indicators due to the fact that they possess sharp resonances at lower energies. The lowest resonance energies are 4.28 eV for tantalum and 4.15 eV for tungsten. Unnecessary thermal and cold neutrons were eliminated by a cadmium filter, and the T_0 and disk choppers were not used. The distance from the neutron source to the detector was about 24 m, and the neutron shutter and the rotary collimators were set to provide the highest neutron intensity (L/D was 240). The neutron beam was collimated to about 55 x 55 mm^2 just upstream of the sample by boron-containing polyethylene blocks. Figure 3 (center) shows the two-dimensional distribution of transmitted neutrons between 4.14 and 4.29 eV covering both resonances of tantalum and tungsten.

The tantalum and tungsten sheets were set inside a vacuum quartz tube (inner diameter: ca. 36 mm) of a furnace (Fig. 3 (right)) having an Inconel heater surrounded by a gold-coated reflector. The measurements were performed at heater temperatures of room temperature, 100, 200 and 300 degrees Celsius. The temperature of the samples was monitored with a thermocouple attached at the center of the tungsten sheet. The average sample temperature during the room temperature measurement, when the furnace was not turned on, was 25.5℃, changing from 23.5℃ to 30.5℃. The temperatures of other cases were 96.1±0.2℃, 189.0±0.1℃ and 285.5±0.1℃. These errors are due to temperature variations during the measurements.

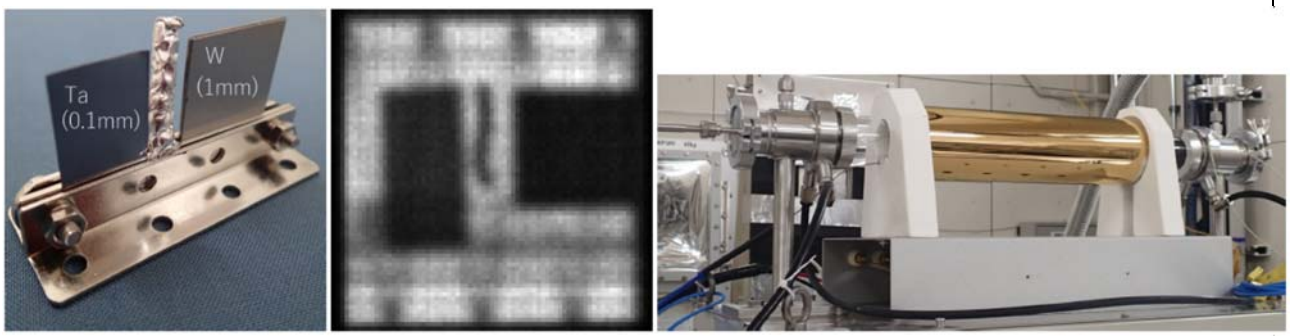

Figure 3 Tantalum and tungsten sheets (left), transmission image of neutrons between 4.14 and 4.29 eV (center) and photograph of furnace (right).

【Preliminary Result】

Figure 4 shows the neutron counting rates at the positions of the tantalum and tungsten indicators as a function of neutron energy. The regions of the indicators were found by the resonance absorption image as shown in Fig. 3 (center), and the selected area of the tantalum and tungsten indicators were 1.2 and 2.1 cm^2, respectively. The regions covered by the sample holder were not included. Only the neutron intensities at 26℃ and 285℃ were plotted in the Fig. 4 for easy discrimination. Those at 96 ℃ and 189℃ were in between them. The broadening of the resonance dips with temperature increase was clearly recognized in both indicator cases. Regions of interest were set in sides of the resonance dips. The correlation between neutron intensity in the regions of interest and temperature will be discussed.

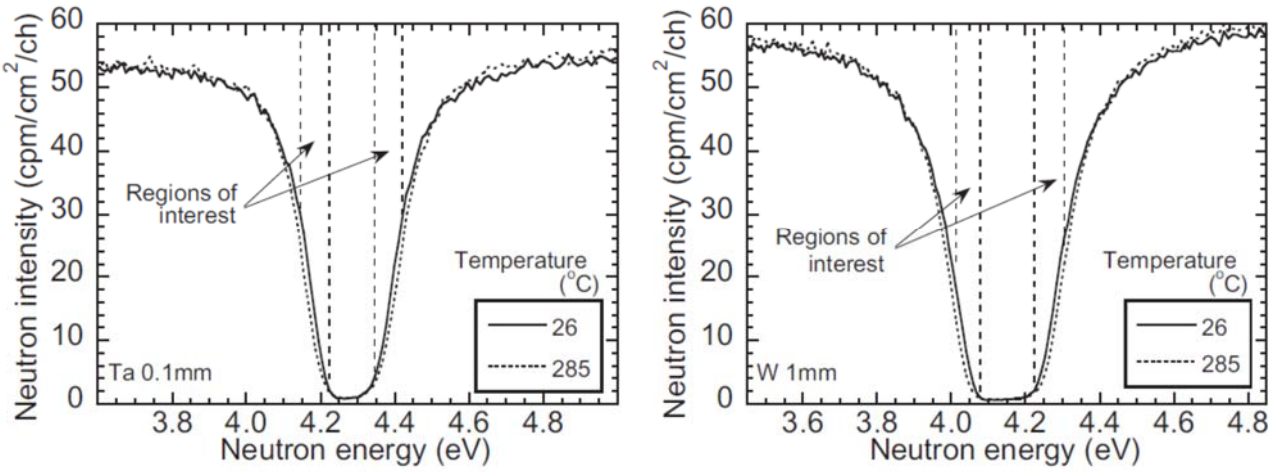

Figure 4 Neutron intensities at resonances of tantalum (left) and tungsten (right). Only those at 26℃ and 285℃ are shown for easy discrimination. Those at 96℃ and 189℃ are in-between.

This work is partially supported by Photon and Quantum Basic Research Coordinated Development Program from the Ministry of Education, Culture, Sports, Science and Technology, Japan.

III. Magnetic Field Imaging

【Purpose】

The purpose of this experiment is a test experiment to quantify a strong magnetic field in a model motor using polarized pulsed neutron imaging.

【Background】

We have been developing a quantitative magnetic field imaging technique for three years using polarized pulsed neutrons and trying to quantify a magnetic field in a model motor that is a test sample of industrial products. According to the computational simulation of a magnetic field in the motor, integrated field strength at the gap between a rotor and a stator of the motor is estimated to be 0.5～2.5 T·mm. To quantify such a strong field using polarization analysis, we have to use thermal neutrons around 2～3 Å. The polarizer and the analyzer installed at RADEN are designed to polarize neutrons with wavelength longer than 1.5 Å and we can analyze wavelength dependent polarization with such a shorter wavelength neutron. In this experiment, we tried to quantify the strong magnetic field in the model motor with the polarization imaging apparatus at RADEN.

【Experiment】

The polarized pulsed neutron imaging was performed using polarization analysis apparatus at BL22 RADEN. Figure 5 shows photos of the polarization analysis apparatus of RADEN. The μPIC-based Neutron Imaging Detector (μNID) was used as a detector that is located at the upstream detector position where distance from the neutron source was 18.5 m. Model motor was located at sample space in the magnetic shielding chamber. A distance between neutron source and the sample was 17.5 m. We measured two kinds of neutron transmission image with the spin flipper off (I_{off}) and on (I_{on}), and then obtained polarization image P by calculating $P = (I_{off} - I_{on})/ (I_{off} + I_{on})$. The exposure time for obtaining a neutron transmission image was 15 hours.

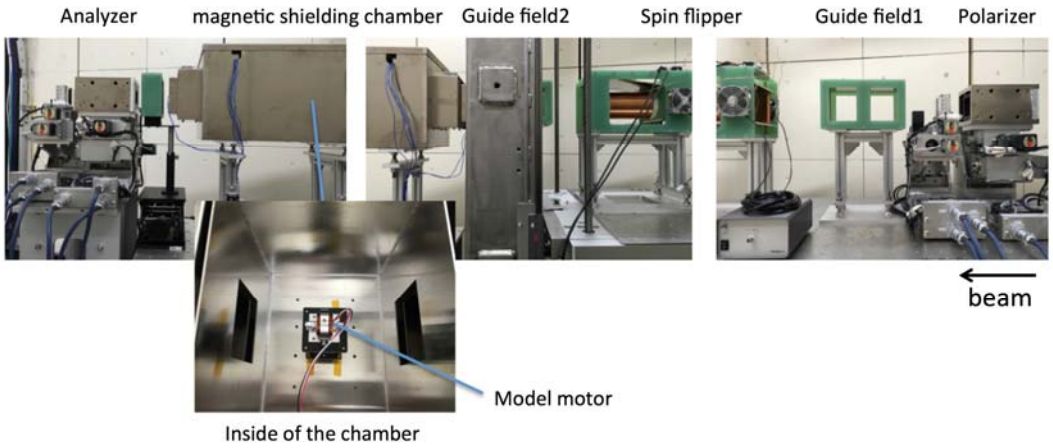

Figure 5. Setup of the polarization imaging experiment at RADEN.

【Preliminary Result】

Figure 6 shows obtained polarization image of the model motor and wavelength dependent polarization in several positions. A direction of quantized axis of polarized neutrons was parallel to Y-axis. As is shown in this figure, oscillatory behavior in wavelength dependence of polarization was not observed at the gap position of the motor. There is possibility that polarization oscillation smeared because field variation in the motor is too fine to analyze with present spatial resolution of the detector. We are now checking a field strength distribution in the model motor using a field simulation.

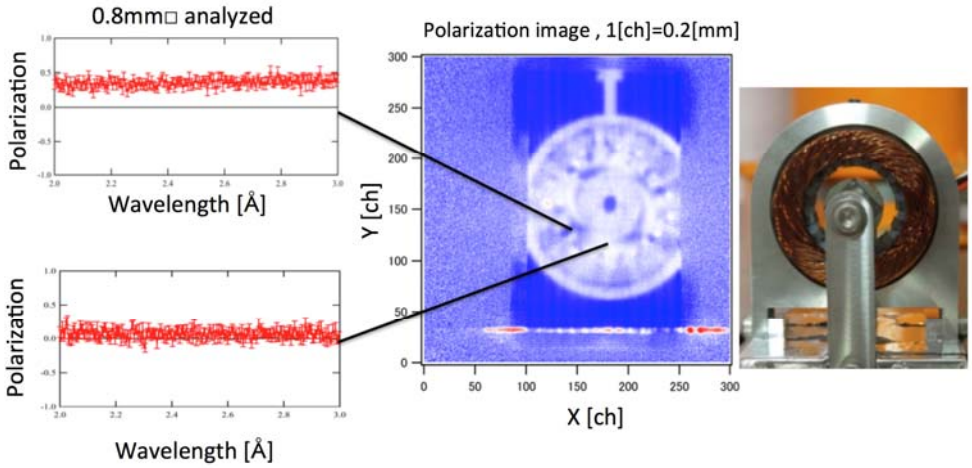

Figure 6. Polarization image of the model motor and wavelength dependent polarization in several positions.

This work is partially supported by Photon and Quantum Basic Research Coordinated Development Program from the Ministry of Education, Culture, Sports, Science and Technology, Japan.

Please use A4-size paper for further reporting, if necessary.